2010

CFD Analysis of Discharge Gas flow in Rotary Compressor for OCR reduction

Kamal Sharma
Tecumseh Product India Pvt Limited

Koteswara Rao
Tecumseh Product India Pvt Limited

Kiran M. N. S/ V
Tecumseh Product India Pvt Limited

Anil Gopinathan
Tecumseh Product India Pvt Limited

CFD Analysis of Discharge Gas flow in Rotary Compressor for OCR Reduction

Kamal Sharma, V. Koteswara Rao, M N S V Kiran, Anil Gopinathan

Tecumseh Product India Pvt. Limited, Product Engineering Department, Balanagar Township,

Hyderabad, 500037, Andhra Pradesh, India

Tel: +91-40-23078103-106, +91-40-23074965, Fax: +91-40-23074965

Kamal.Sharma@tecumseh.com, koteswararao.vaddadi@tecumseh.com, Kiran.Mnsv@tecumseh.com, Anil.Gopinathan@tecumseh.com

ABSTRACT

This paper presents the use of CFD as a design tool in the development of rotary compressor for the purpose of reduction in Oil Circulation Rate (OCR). In the present work, CFD analysis is done using a commercial CFD package to simulate the discharge gas flow within the rotary compressor. Discharge gas flow path in the compressor is redefined by providing features that support OCR reduction.

One such feature is providing a few holes in the stator lamination. The no of holes, size and locations are optimized for similar motor performance as that of original design with the help of electromagnetic Simulation packages.

The effect of hole- in-stator design on gas flow is evaluated using CFD and is further optimized for improved gas flow in terms of flow velocities and pressure drop at various sections inside the compressor to achieve reduction in OCR.

Prototype compressors were built and tested, the practical performance in terms of OCR is in line with the CFD study.

1. INTRODUCTION

The lubricating oil charged in a hermetic compressor is a necessary ingredient as it provides not only lubrication to the moving parts (vane, Roller, shaft in bearings) but also serves as a medium to remove heat generated from gas compression, mechanical rubbing of parts, motor, etc and to transfer it to the compressor shell. In the high side Rotary compressor, the gas inside the compressor shell is a compressed gas at high pressure and temperature. This discharged gas, which is exposed to lubricating oil, is prone to carry some oil with it to the air-conditioning system where excess oil is accumulated in the condenser coils, expansion valves and evaporator coils. The heat transfer characteristics of condenser and evaporator are changed due to this “accumulated” oil and system performance (or efficiency) is deteriorated.

Oil Circulation Rate (OCR) is a measure of this carryover of lubricating oil by the discharge gas and is an indicator of reliable and efficient functioning of a hermetic compressor as well as of the air-conditioning system.

Min and Hwang (2000) discussed the method of measuring OCR that are suitable for compressor manufacturer (Weight Measurement Method in which OCR is measured as weight % of oil in the mixture of oil and gas) as well as for OEMs (Oil Separating Method that requires an oil separator and OCR is measured in cc/min (or lb/hr).

Higher OCR means large amount of oil is carried by gas and is seen as “loss” of oil for a compressor. TOYAMA *et al.* (2006) discussed the effects of high OCR. Considering these “negative” effects of high OCR, OCR should be kept at minimum possible level.

Inside the rotary compressor shell, the oil forms a mist state in which oil droplets are suspended in the discharge gas. These droplets are of various sizes and distribution densities. TOYAMA *et al.* (2006) discussed the visualization and behavior of these oil droplets in scroll compressor whereas Yong-Jae KIM *et al.* (2004) investigated and visualized the oil droplets in Rotary Compressor.

Oil discharge mechanism (the mechanism of oil carryover by discharge gas) consists of "source", "path" and "collectors" components in rotary compressor (Paul Bushnell, 1996). "Sources" (e.g. oil sump level, vane and spring activities, discharge gas leakage into oil sump through muffler – short bearing hub clearance, rotor windage, radial hole in shaft at the main bearing etc) are responsible for distribution density of oil droplets, their sizes as well as oil concentration of oil in oil-gas mixture. Whereas "paths" (e.g. stator core cut area, air gap, rotor vent hole, discharge tube, etc) affect the velocities of oil droplets flowing with the discharge gas. Collectors (e.g. shell inner surface, stator slots, motor windings, rotor cover plate, etc) affect the size of the droplets and help in draining of oil from the mist.

Discharge gas velocities and turbulence are importance factors that affect the formation, carryover and collapsing of oil droplets. The importance of gas velocities lies in the mechanism of droplet generation (dispersion mechanism) and droplet collapse (separation mechanism). When the relative velocity between oil and gas is sufficiently large, the interfacial shear stress produces waves on the interface and the breakup of the waves generates a spray of oil droplets that is transported further into the gas phase by the turbulent motions. This is similar to the hurricane generated ocean spray. This happens in the case when gas is released from the top muffler from which it flows over the oil sump as well as the all the wetted surfaces. In the case when gas is discharged from the bottom side muffler (due the leakage) into the oil sump, the oil spray is generated by process of break-through. This leaked gas forms the gas bubbles that rise to break through the free surface of oil. This leakage of gas becomes crucial when leakage rate is high (e.g high capacity compressor or compressors running at very high speed). This leakage makes the oil sump motion very violent and the oil spray is formed within the gas bubbles. This spray is then released when the bubbles reach the surface of oil sump. The churn-turbulent flow by the rotation of crankshaft in the oil sump too adds up to this phenomenon.

The relationship between the gas velocities and oil droplets can be defined by the drag law:
Let R is the droplet radius, ν_{gas} and $\rho_{gas}$are the kinematic viscosity and density of discharge gas, ρ_{oil} is the density of oil droplets. C_D is coefficient of drag and g is acceleration due to gravity. V_l is the absolute droplet velocity and V_r is the relative droplet velocity $(= V_l - V_{gas})$.

$$m\frac{dV_l}{dt} = \frac{C_D}{2}\rho_{gas}\pi R^2|V_r|(-V_r) \tag{1}$$

Where, m is the droplet mass, given by:

$$m = \left(\frac{4}{3}\pi R^3\right)\,\rho_{oil} \tag{2}$$

For Stokes flow of low Reynolds number $(Re\ \leq 1)$,$C_D = \frac{24}{Re}$.
Buoyancy force and gravity forces may be added to drag force at right side of equation (1) in the case of motion of rigid sphere moving in quiescent fluid.

Every droplet has a terminal velocity (or Settling velocity or Separation velocity for two-phase mixture of droplets and gas). For a particular size of droplet, the separation velocity can be calculated by following equation.

$$W_{droplet} = \frac{2R^2g}{9\nu_{gas}}\frac{(\rho_{oil}-\rho_{gas})}{\rho_{gas}}, \quad \text{if } Re_{droplet}\left(= \frac{2R\,W_{droplet}}{\nu_{gas}}\right) \ll 1 \tag{3}$$

Or,

$$W_{droplet} = \left\{\frac{2Rg}{3C_D}\frac{(\rho_{oil}-\rho_{gas})}{\rho_{gas}}\right\}^{\frac{1}{2}}, \quad \text{if } Re_{droplet}\left(= \frac{2R\,W_{droplet}}{\nu_{gas}}\right) \gg 1 \tag{4}$$

When the gas velocity exceeds this Separation velocity of a particular size oil droplet, droplet is carried by the gas otherwise it is settled to the collector surface or to the oil sump. The larger size droplets are settled easily while small size droplets are carried by the gas. Therefore, controlling the gas velocities and its turbulence is crucial for reducing OCR.

Due to recent development of CFD (Computational Fluid Dynamics) beyond academic research as well as popular aero/automotive industry applications, it is understood to be a good alternative of DOE experiments. Once a CFD analysis method for a particular application is validated by experimental data, it can be used for comparative analysis of various designs, cutting down the cost and time of prototype development. It is also a good tool to visualize and understand the complex behavior of fluid flow and gas-liquid-solid interactions. Based on this knowledge, the products can be improved further for better performance which is otherwise limited by experimental study. The usage of CFD in the hermetic compressor is also advantageous keeping in mind that it is sealed container and it can be quite difficult and costly to visualize or inspect the gas flow, formation of oil mist and behavior of oil droplets in working condition.

2. OVERVIEW OF CURRENT WORK

Hole-in-stator is a design concept that effect positively on the OCR. Holes provide more gas flow area through the stator and so may reduce the gas flow velocities in the upper part of shell. Also, the interior surfaces of pipes formed by these holes in stator stack act as collector for oil.

The design of the holes in stator is not only important for gas flow but also for the motor performance. Holes may alter the flux distribution of the stator core, may affect core losses and consequently, the motor efficiency. Therefore various configurations of holes were analyzed for the electrical performance first, using a commercial electromagnetic package JRI JMAG. Then optimized design was chosen and compared with without-hole design for gas flow in ANSYS CFX. Then prototype compressors were built up to evaluate final design configuration.

2.1 Design Configurations:

Table 1 : Various design configurations used in analysis:

Sl.	Design Code	Design		PCD (mm)	No of Holes	Hole dia (mm)	Electromagnetic Analysis	CFD Analysis	Experimental Verification
1	VH-0	Without Hole	Baseline	--	0	--	✔	✔	✔
2	VH-1	With Holes	Trial	140.8	12	4.0	✔	✔	✔
3	VH-2	With Holes	Trial	140.8	16	2.5	✔	✕	✕
4	VH-3	With Holes	Trial	135	12	4.0	✔	✕	✕
5	VH-4	With Holes	Trial	135	16	2.5	✔	✕	✕

3. ELECTROMAGNETIC ANALYSIS

The single phase induction motor (stator and rotor) was analyzed for various configurations of hole-in-stator designs, using JRI JMAG electromagnetic package. 2D CAD models are shown in the Figure 1. The outer dia of the stator was 5.9” (149.86mm) and outer dia of rotor was 2.6” (66.35mm). Stack height of stator was 3.75” (95.25mm). Input voltage was 230V and frequency was 50Hz. Figure 2 shows the JCF files and Mesh models used in JMAG.

3.1 CAD Models, JCF Files, Mesh Mdoels:

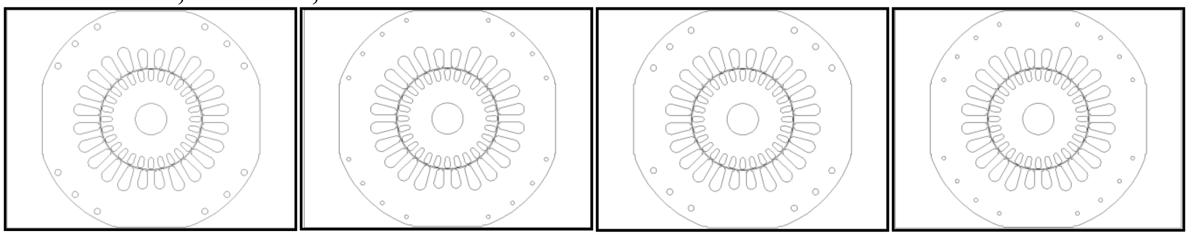

(VH-1) (VH-2) (VH-3) (VH-4)

Figure 1: 2D models of various design configurations for electromagnetic analysis

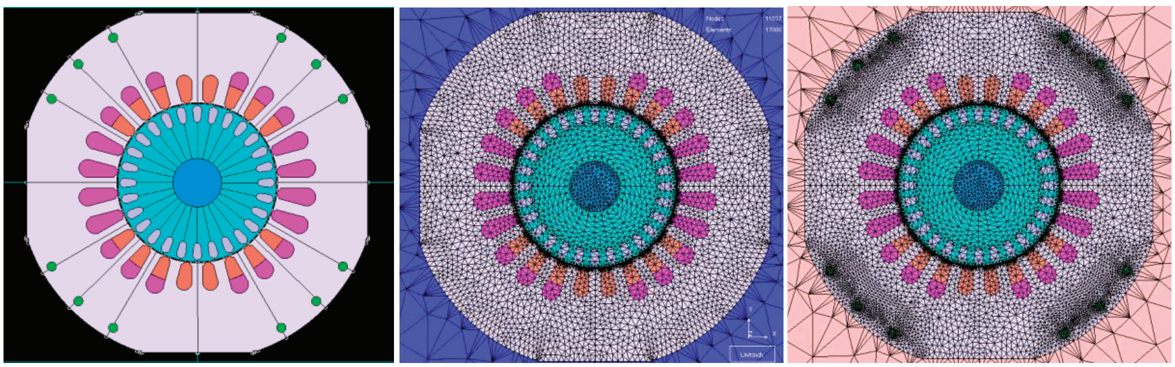

(a) (b) (c)

Figure 2: JCF (a) and Mesh models of without-hole design (b) and holes-in-stator designs (c)

3.2 Analysis Results:

All the cases were run at the same speed and comparison of the results are in the Table 2:

Table 2: Electromagnetic analysis results comparison:

	Design Cases	**VH-0**	**VH-1**	**VH-2**	**VH-3**	**VH-4**
Electrical Parameters	**Units**	**Without-Hole**	**140.8mm PCD, 4 mm dia, 12Nos**	**140.8 PCD, 2.5 mm dia, 16 Nos**	**135mm PCD, 4 mm dia, 12 Nos**	**135mm PCD, 2.5 mm dia, 16 Nos**
Speed	RPM	2927	2927	2927	2927	2927
Torque	Oz-ft	85.36	85.85	85.29	86.01	85.89
Input	W	2217.2	2230.0	2215.6	2234.1	2231.1
Output	W	2138.9	2152.8	2166.8	2156.7	2140.9
Output + Total Losses	W	2566.9	2598.0	2575.3	2595.0	2590.5
Efficiency	(%)	86.4	85.8	86.0	86.1	86.1
Iron loss	W	84.40	92.42	92.77	90.38	90.99

It can be seen in above comparison that, there is loss of motor efficiency when holes are added to the stator. But this loss in efficiency is negligible. Among the all other design configurations, the 135mm PCD has higher efficiency as well as lower iron losses.

The magnetic flux lines and flux distribution is compared in Figure 3. It can be seen that, the 140mm PCD holes are in the blue regions where flux density is very low, whereas the 135mm PCD holes are within the higher flux density region and the flux lines cut across the holes. Localized flux distribution around the holes can be seen in VH-3 and VH-4 designs. So 140mm PCD design is preferred over 135mm PCD design. 4mm dia holes are preferred over 2.5mm dia holes for ease in manufacturing (punching of laminations), tooling, etc.

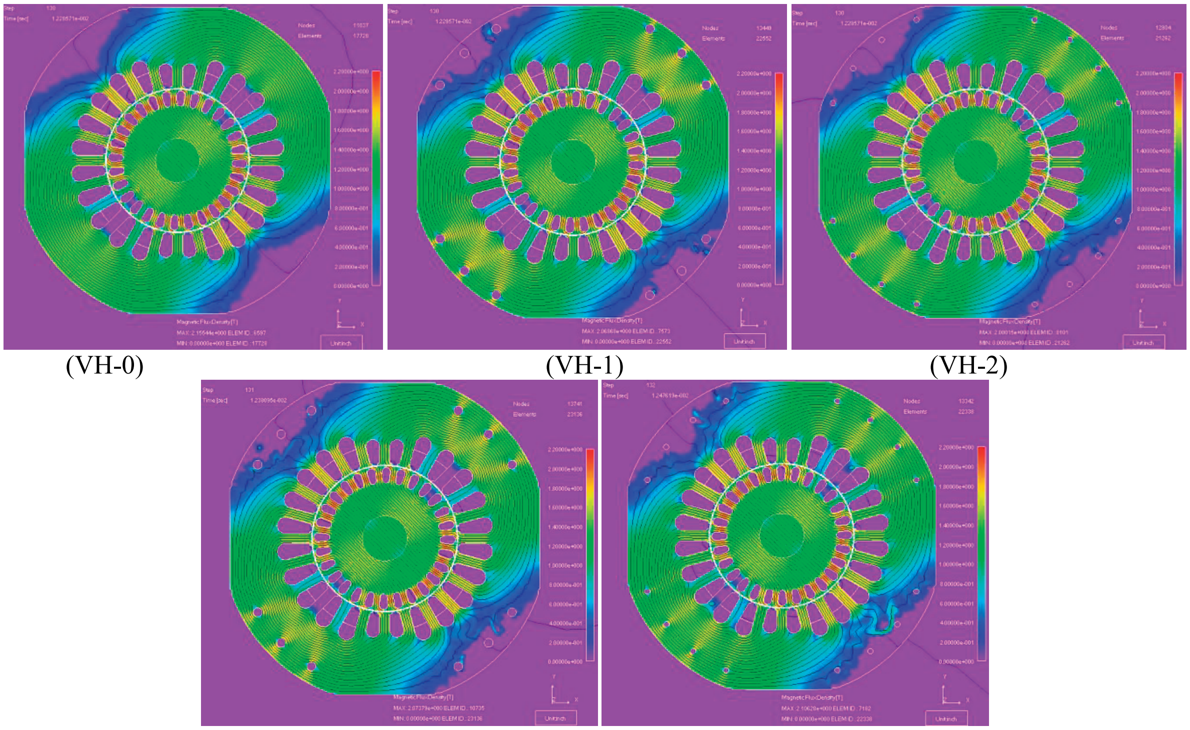

(VH-0) (VH-1) (VH-2)

(VH-3) (VH-4)

Figure 3: Magnetic Flux density and flux lines comparison

Torque curves comparison is shown in the Figure 3. It can be seen that in all the cases, torque variation with respect to time almost same.

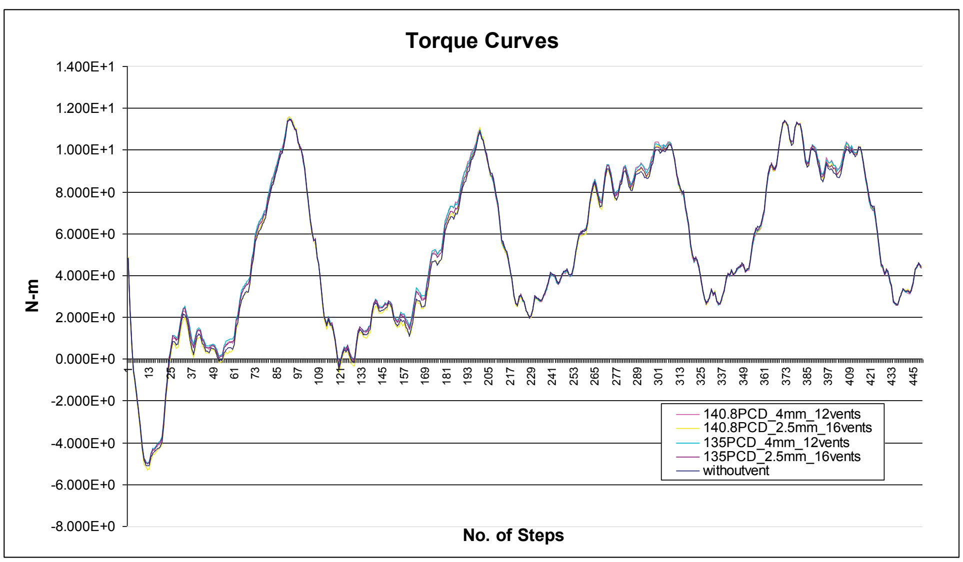

Figure 4: Torque variation *w.r.to* time:

From the above analysis results, the 140mm PCD, 4 mm hole, 12 nos of holes design (CH-1) was chosen for CFD Analysis anc compared with without-hole design (VH-0).

4. CFD ANALYSIS

4.1 Construction of rotary compressor and fluid volume:

Figure 5(a) shows the sectional view of a rotary (Rolling piston type) compressor. The low temperature and low pressure gas from evaporator is inhaled by cylinder block through accumulator. There, the gas is compressed in the compression chamber formed by the rolling piston and cylinder bore. This high temperature and high pressure discharge gas is released inside the compressor shell through top side muffler. The sectional view of shell cavity fluid volume is shown in the Figure 5(b). The discharge gas then turbulated by windage created by rotating rotor & bottom counterweight assembly. This gas is then passes over the bottom side stator winding, and then travel through the slots created by round shaped compressor shell and square shaped stator. Beyond stator, this gas once again passes over top side of stator winding , getting turbulated by windage of rotor and top counterweight assembly, and then finally released out of compressor through discharge tube. ANSYS CFX was used for CFD analysis and ANSYS ICEM CFD was used for tetrahedral mesh generation of fluid volume. Fluid volume was trimmed to the Main bearing bottom surface assuming the oil sump level up to this mark.

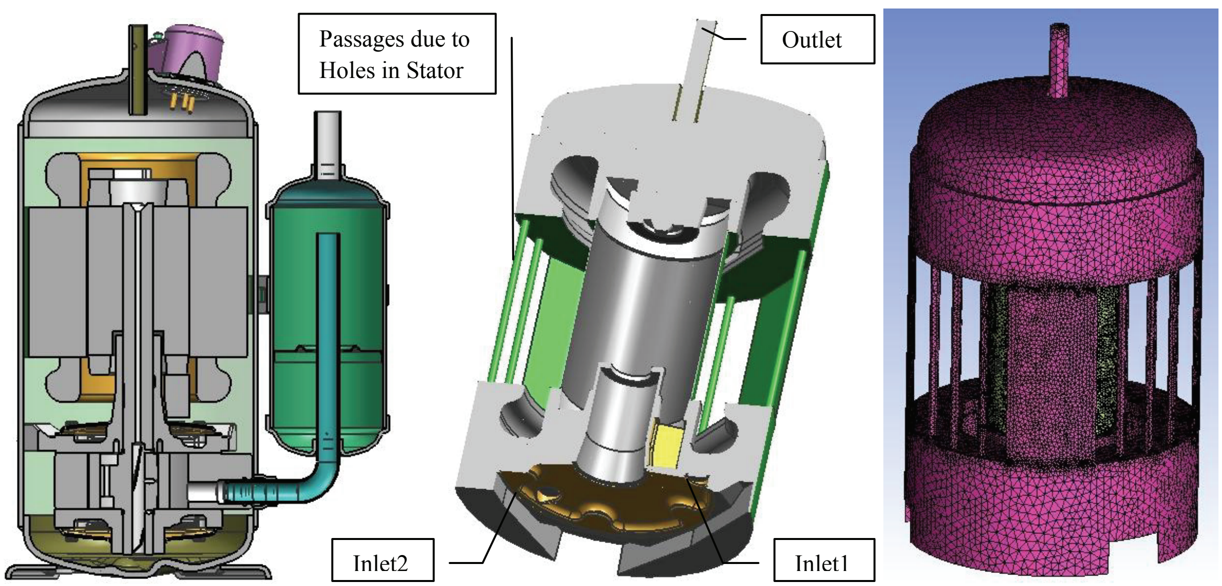

(a) (b) (c)

Figure 5: (a) Sectional View of Rotary Compressor, (b) Sectional view of Fluid Volume, (c) Mesh Model

4.2 Mesh

The finite volume mesh of analysis domain is shown in the Figure 5(c). Total 520,710 elements were generated in the case of without-hole stator design (VH-0) and 535,200 tetrahedral elements were generated in the case of holes-in-stator design (VH-1).

4.3 Boundary Conditions

A steady state analysis of single phase R22 refrigerant was performed. A non-buoyant stationary fluid domain (Shown in Fig5(b)), filled with R22 refrigerant gas at 105 ^{o}C temperature was assumed. Redlich Kwong model was used for R22 for the calculation of refrigerant properties. The two ports of the top muffler through which this gas is released were termed as “INLET1” and “INLET2”, as they are inlets to the shell cavity fluid volume. The gas exit area of discharge tube was termed as “OUTLET”. At both the inlets, mass flow rate of 0.0217 kg/s each was defined whereas at the “OUTLET”, static pressure of 2046.92 kPa (296.88 psi) of gauge pressure was defined with 101.353 kPa (14.7 psi) as reference pressure. Rotor and counterweights assembly were given rotating walls with 2900 RPM. k-ε turbulence model with turbulent eddy dissipation was used.

4.4 Analysis Results:

The streamlines varying with velocity magnitude is plotted and contour plots of velocity and pressure at the vertical sectional plane are also shown in the Figure 6 and 7.

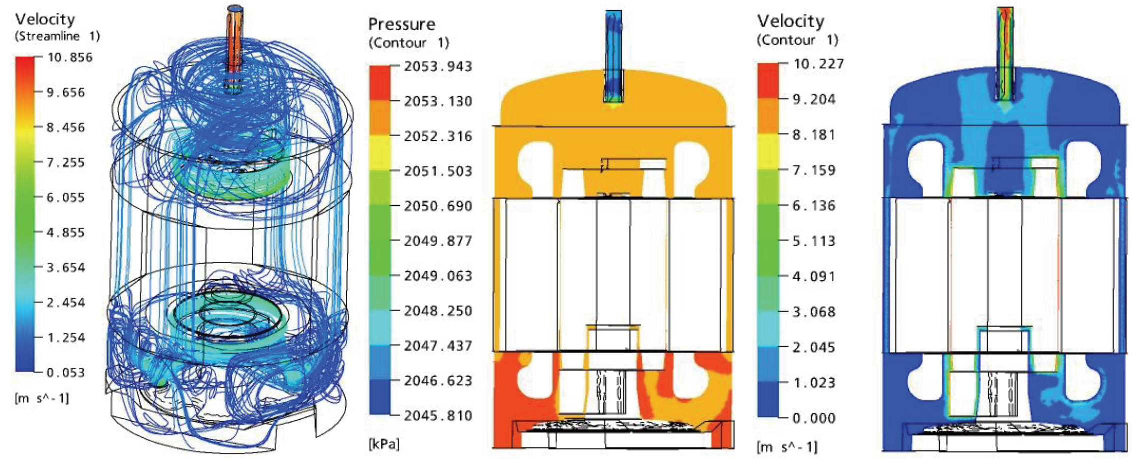

Figure 6: Without-hole Design (VH-0):
(a) Streamlines vary with velocity magnitudes, (b) Pressure Contour, (c) Velocity Contours

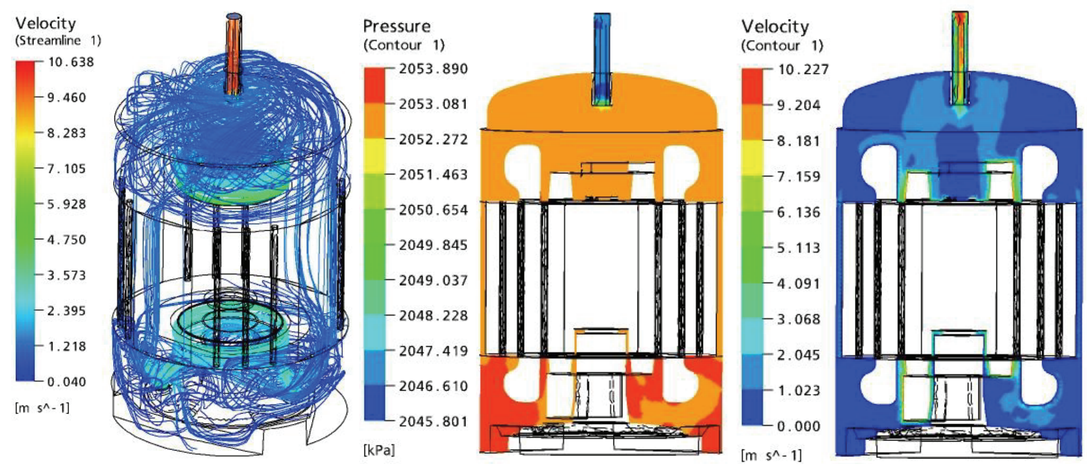

Figure 7: Hole-in-stator Design (VH-1):
(a) Streamlines vary with velocity magnitudes, (b) Pressure Contour, (c) Velocity Contours

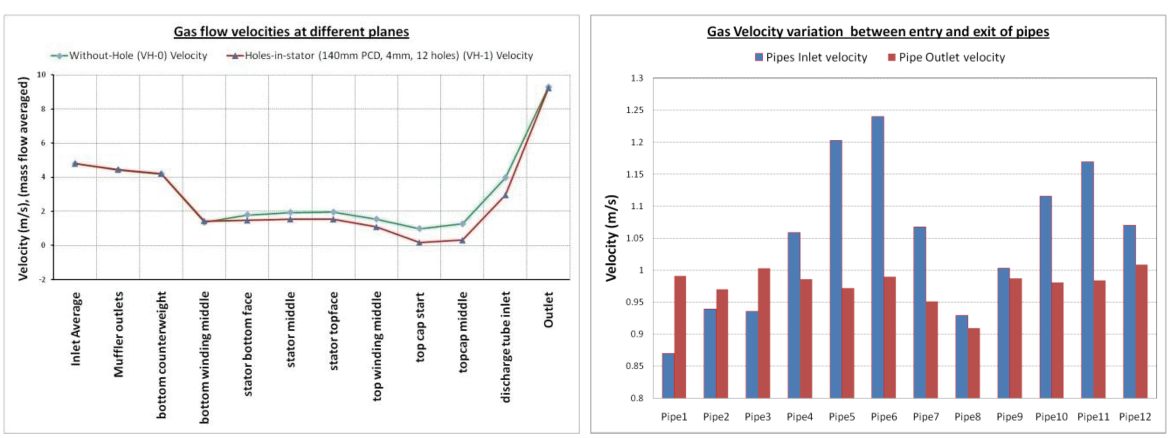

Figure 8: Gas velocity comparison (a) at different planes (b) between entry and exit of pipes

To understand the gas velocity variation in the shell along the gas flow path, 10 parallel planes were created at various locations of interests along the Vertical direction. The gas velocities at these planes were measured and compared in the two cases (Figure 8(a)). It can be seen that, as predicted, the gas velocities are decreased not only in the stator but also in the top shell region. In Figure 8(b), gas velocities of various pipes formed by the holes in stator stack are compared. It can be seen that, due to the locations of pipes, the gas velocities vary at the entries of these pipes. However, at the exit, the velocities are more uniform in nature. That means, gas flowing out of stator is now uniformly distributed along the stator periphery. It was found that average pressure drop in the pipes was 42 Pa, which is very low as compare to operating pressure. However, in practical, this pressure drop may be more due to high friction factor caused by stacked stator laminations as well as oil-gas two-phase flow in these small dia pipes. The overall pressure drop from inlet to outlet was found to be about 4450 Pa, which is about 0.2% of inlet average pressure of 2053 Pa.

5. EXPERIMENTAL ANALYSIS

Prototype compressors were built-up to compare the without-hole and hole-in-stator designs. The OCR was measured and compared. Table below shows the summary of tested compressor data:

Design	**Design code**	**OCR (% w/w)**
Without-hole design	VH-0	3.26
Hole-in-stator design	VH- 1	1.23

6. CONCLUSION

It is understood that, gas velocities and turbulence in the Rotary compressor are important for the oil droplets dispersion and separation and are important for reducing OCR. Among the various methods of reducing the gas velocity & turbulence and oil separation from gas-oil mixture, the hole-in-stator design was taken for study of gas flow in the compressor shell. First, hole-in-stator design was optimized by electromagnetic analysis of various hole configurations and also by manufacturing considerations. Then the chosen design was analyzed for gas flow using CFD. The gas velocities were compared with without-hole design at various planes along the gas flow path. These were found to be in-line with the prediction. Later the prototype compressors were built and tested with the chosen design to verify the reduction in OCR from 3.26% (w/w) to 1.23% (w/w). CFD analysis helped in understanding flow behavior in the otherwise sealed compressor, which later helped in reducing OCR further by incorporating other OCR reduction features in the compressor. The discussion about those feature and their CFD analysis are out of the scope of this paper.

REFERENCES

Bushnell Paul, “Oil Droplet Generation and control in Rolling Piston Type Compressors”, *International Purdue Engineering conference at Purdue*, 1996, pp 335-340

Kyungki Min, Insoo Hwang, “Oil Circulation Rate in Rotary Compressor: Its measurement and factors affecting the Rate”, *International Purdue Engineering conference at Purdue*, 2000, pp 269-274

Toshiyuki TOYAMA, Hideki MATSUURA, Yoshiaki YOSHIDA, “Visual Techniques to quantify behavior of oil droplets in a scroll compressor”, *International Purdue Engineering conference at Purdue*, 2006, C026

Takeshi Ogata, Hiroshi Hasegawa, Atsuo Okaichi, Fumitoshi Nishiwaki, “Reduction of oil discharge for Rolling Piston Compressor using CO_2 Refrigerant”, *International Purdue Engineering conference at Purdue*, 2006, C095

Yong-Jae KIM, Seung-Kap LEE, Young YOUN, Han Seo KO, “Experimental study of refrigerant –oil behavior inside Rotary compressor”, *International Purdue Engineering conference at Purdue*, 2004, C046